T98/070

New Integrable Lattice Models From Fuss-Catalan Algebras

P. Di Francesco*,

Department of Mathematics,
University of North Carolina at Chapel Hill,
CHAPEL HILL, N.C. 27599-3250, U.S.A.,

and

Service de Physique Théorique,
C.E.A. Saclay,
F-91191 Gif-sur-Yvette Cedex, FRANCE.

We construct new hyperbolic solutions of the Yang-Baxter equation, using the Fuss-Catalan algebras, a set of multi-colored versions of the Temperley-Lieb algebra, recently introduced by Bisch and Jones. These lead to new two-dimensional integrable lattice models, describing dense gases of colored loops.

07/98

* e-mail: philippe@math.unc.edu

1. Introduction

The Yang-Baxter equation [1] plays a central role in the definition of two-dimensional integrable lattice models. It is a sufficient condition on the matrix of Boltzmann weights of the statistical model ensuring integrability. Each of its solutions indeed leads to an infinite family of commuting transfer matrices, which should simultaneously diagonalize in a Bethe-Ansatz-type basis. Solutions with additive spectral parameters are of three types: elliptic, trigonometric (or hyperbolic) and rational, referring to the type of functions of the spectral parameter involved in the definition of the Boltzmann weights, each type leading to the next by some limiting process.

In this paper, we concentrate on hyperbolic solutions. Among the many known constructions, the most systematic seems to be to associate a solution to any multiplicity-free tensor product of two representations of an affine quantum algebra $\mathcal{U}_q(\widehat{G})$, G any classical Lie algebra [2][3]. The simplest example of this uses two spin-$\frac{1}{2}$ representations of $\mathcal{U}_q(\widehat{sl}_2)$, and leads to the XXZ quantum spin chain or the equivalent 6 Vertex model [4]. This solution actually arose from Baxter's study of the equivalence between the 6 Vertex model and the critical Q-states Potts model, in which he found the matrix of Boltzmann weights to be of the form $W_i(u) = 1_i + a(u)U_i$, u the spectral parameter, where U_i form a matrix representation of the Temperley-Lieb algebra $TL_n(\beta)$ [1] [5], with $\beta = \sqrt{Q}$.

The Temperley-Lieb algebra has a simple pictorial representation which makes it ideal for describing a dense loop model on the square lattice, with a fugacity β per loop. This representation has also become a basic tool in the definition of link polynomials [7]. A relation with meanders [8], i.e. compact folding configurations of polymer chains has also been found [9], using the same representation.

The Temperley-Lieb algebra has been recently generalized by Bisch and Jones [10], by introducing a multi-colored version of the above pictorial representation. The resulting algebras are called the k-color Fuss-Catalan algebras, denoted by $FC_n(\alpha_1, \alpha_2, \ldots, \alpha_k)$. In the particular case $k = 2$, the authors have given an explicit presentation of $FC_n(\alpha, \beta)$ in terms of generators and relations.

In this paper, we use the k-color Fuss-Catalan algebras to construct new hyperbolic solutions to the Yang-Baxter equation. The corresponding statistical models describe multi-colored dense loops with specific fugacities.

The paper is organized as follows. We start by recalling in Sect.2 some known facts about the one-projector hyperbolic solutions to the Yang-Baxter equation, and their link with the Hecke algebra, of which the Temperley-Lieb algebra is simply the particular quotient corresponding to the commutant of $\mathcal{U}_q(\widehat{sl}_2)$. In Sect.3, we solve the Yang-Baxter equation, looking for a matrix of Boltzmann weights which is a linear combination of the generators of $FC_n(\alpha,\beta)$, with coefficients function of the spectral parameter. This is possible only if $\alpha=\beta$ and leads to the definition of a dense two-loop model on the square lattice. In Sect.4, we generalize this to the case of an arbitrary k-color Fuss-Catalan algebra, for which we first give a presentation with generators and relations. We find a number of solutions, indexed by a set of "spins" $r_i \in \{\pm 1\}$, $i=2,4,\ldots,k-2$, $r_i=r_{k-i}$. These lead to integrable multi-colored dense loop models, with specific fugacities. Sect.5 is devoted to a discussion of our solutions and concludes with a list of open questions to be addressed.

2. Hyperbolic Solutions To The Yang-Baxter Equation

2.1. Vertex Models And The Yang-Baxter Equation

The Yang-Baxter equation is a sufficient condition for ensuring the existence of an infinite set of commuting transfer matrices for a given two-dimensional statistical model. In this work, we will consider only square lattice vertex models. Let us consider a rectangle R containing $N \times M$ vertices and, say E edges numbered $1,2,\ldots,E$. A configuration of the model is a map σ from this set of edges to $\mathcal{T}^{\otimes E}$, $\mathcal{T}$ a finite "'target" set. The weight of such a configuration is a product over all the vertices of R of the vertex Boltzmann weights

$w(i,j|k,m) =$

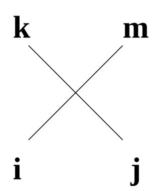

(2.1)

where i,j,k,m denote the images of the four edges of the vertex. The quantities of interest are statistical sums, such as the partition function

$$Z = \sum_{\text{configurations}} \prod_{\text{vertices}} w(i,j|k,m) \tag{2.2}$$

The target $\mathcal{T}$ being finite, it is useful to trade it for a vector space V of dimension $n=|\mathcal{T}|$, with a distinguished basis $\{e_1,\ldots,e_n\}$ in bijection with the elements of $\mathcal{T}$. We may then view the boltzmann weights (2.1) as the matrix elements of a linear operator $W : V \otimes V \to V \otimes V$, acting from top to bottom, namely

$$W e_k \otimes e_m = \sum_{i,j} w(i,j|k,m)\ e_i \otimes e_j \tag{2.3}$$

The operator W may act on a line of $N+1$ edges $V \otimes V \otimes \ldots \otimes V$, as the identity on all spaces except on two of them, say in positions (r,s), where it acts as in (2.3). We will denote $W_{r,s}$ the corresponding operator, and $W_i = W_{i,i+1}$. The monodromy matrix of the model is defined as

$$\mathcal{M} = W_1 W_2 \ldots W_N \tag{2.4}$$

and the transfer matrix T is simply the trace of $\mathcal{M}$, viewed as a linear operator from V_{N+1} to V_1. It is now clear that, if we impose doubly periodic conditions along the bordering edges of R, the resulting partition function reads

$$Z = \mathrm{Tr}(T^M) \tag{2.5}$$

and that the diagonalization of T allows for solving the model completely.

The Yang-Baxter equation is a sufficient condition for the existence of an infinite set of commuting transfer matrices $T(x)$, x a real parameter entering the definition of the Boltzmann weights (2.1). When the T's are diagonalizable,this in turn grants the existence of a common basis of eigenvectors for all the $T(x)$, which can be found by Bethe Ansatz techniques. The Yang-Baxter equation reads:

$$\boxed{W_i(x)W_{i+1}(xy)W_i(y) = W_{i+1}(y)W_i(xy)W_{i+1}(x)} \tag{2.6}$$

and is usually supplemented by the normalization condition:

$$\boxed{W_i(x)W_i(\frac{1}{x}) = 1} \tag{2.7}$$

which fixes the gauge $W_i(x) \to f(x)W_i(x)$ up to a factor $\rho(x)$ such that $\rho(x)\rho(1/x) = 1$. Note that both equations (2.6)-(2.7) must hold for $i = 1, 2, \ldots, N$, whereas all operators act on a line of $N+1$ edges $V^{\otimes(N+1)}$ (in particular, 1 stands for the identity $I\otimes\ldots\otimes I$). It is customary to further fix the normalization of W_i by imposing

$$\boxed{W_i(1)=1} \tag{2.8}$$

The solutions of the Yang-Baxter equation are known to be of three types: elliptic, trigonometric (or hyperbolic) and rational, referring to the type of dependence on the spectral parameter u, such that $x=e^u$. Each type degenerates into the next in some limit. Here we will mainly focus on hyperbolic solutions (i.e. involving only rational fractions of x).

2.2. Hyperbolic Solutions: The One-projector Case

Let us determine all solutions to (2.6)(2.7) of the form

$$W_i(x)=1_i+a(x)U_i \tag{2.9}$$

where all the dependence on x is contained in the function $a(x)$, 1 stands for the identity of $V\otimes V$, and U is an endomorphism of $V\otimes V$. The normalization condition (2.7) implies that U satisfies a quadratic equation of the form $\lambda U+\mu U^2=0$, and if U is non-trivial, we must have $U^2=\beta U$. Hence U is an un-normalized projector. Moreover,

$$a(x)+a(\frac{1}{x})+\beta a(x)a(\frac{1}{x})=0 \tag{2.10}$$

It is now easy to write the condition (2.6), which amounts to

$$\begin{aligned}\big(a(x)+a(y)+\beta a(x)a(y)-a(xy)\big)(U_i-U_{i+1})\\ +a(x)a(xy)a(y)(U_iU_{i+1}U_i-U_{i+1}U_iU_{i+1})=0\end{aligned} \tag{2.11}$$

Up to a multiplicative redefinition of β, this implies that $U_iU_{i+1}U_i-U_i=U_{i+1}U_iU_{i+1}-U_{i+1}$, and that

$$a(x)+a(y)+\beta a(x)a(y)+a(xy)\big(1-a(x)a(y)\big)=0 \tag{2.12}$$

Expanding to first order in ϵ, for $y=e^\epsilon/x$, and using $a(1)=0$ from (2.8), we find

$$\frac{1}{x}a'(\frac{1}{x})(1+\beta a(x))+a'(1)(1-a(x)a(\frac{1}{x})=0 \tag{2.13}$$

which, together with (2.10) leads to the differential equation $xa'(x) = -a'(1)(1+\beta a(x)+a(x)^2)$, easily solved as

$$a(x) = \frac{x^\gamma - 1}{z - x^\gamma/z} \tag{2.14}$$

where $z + 1/z = \beta$ and where $\gamma = a'(1)(z - 1/z)$ can be safely set to 1 (which amounts to redefining $x = e^{\gamma u}$).

We conclude that the most general non-trivial solution to (2.6)(2.7)(2.8) of the form (2.9) reads

$$W_i(x) = 1_i + \frac{x-1}{z - \frac{x}{z}} U_i \tag{2.15}$$

where the U's satisfy the following relations

$$\boxed{\begin{aligned} U_i^2 &= \beta U_i \quad i = 1, 2, \ldots, N \\ U_i U_j &= U_j U_i \quad \text{for} \ \ |i-j| > 1 \\ U_i U_{i+1} U_i - U_i &= U_{i+1} U_i U_{i+1} - U_{i+1} \quad i = 1, 2, \ldots, N-1 \end{aligned}} \tag{2.16}$$

The algebra generated by the U_i, $i = 1, \ldots, N$ and the identity 1 is the Hecke algebra $H_{N+1}(\beta)$.

This exercise can be repeated in the case of more projectors, and higher algebras can be found. In this paper, we will present new solutions with arbitrary numbers of projectors.

It is also interesting to note that particular solutions corresponding to quotients of the hecke algebra (obtained by imposing extra relations on the U's) have been found. They correspond to the A_{n-1} models of [11], related to the quantum groups $U_q(\widehat{sl}_n)$. In the remainder of this section, we will concentrate on the first of these quotients, also known as the Temperley-Lieb algebra.

2.3. Temperley-Lieb Algebra, 6 Vertex, Potts And Dense Loop Models

The Temperley-Lieb algebra $TL_{N+1}(\beta)$ is the quotient of the Hecke algebra $H_{N+1}(\beta)$ obtained by imposing the extra relations

$$U_i U_{i+1} U_i = U_i \ \ \text{and} \ \ U_{i+1} U_i U_{i+1} = U_{i+1} \tag{2.17}$$

for $i = 1, 2, \ldots, N-1$. The Temperley-Lieb vertex model, with Boltzmann weights (2.15) involving the generators U_i of $TL_{N+1}(\beta)$ can take many forms, depending on the choice of representation (U, V).

Taking a two-dimensional representation $V = Vect(e_+, e_-)$, and the 4×4 matrix of U acting on $V \otimes V = Vect(e_+e_+, e_+e_-, e_-e_+, e_-e_-)$:

$$U = \begin{pmatrix} 0 & 0 & 0 & 0 \\ 0 & z & 1 & 0 \\ 0 & 1 & \frac{1}{z} & 0 \\ 0 & 0 & 0 & 0 \end{pmatrix} \tag{2.18}$$

we recover the celebrated 6 Vertex model, with parameter $\Delta = -\beta/2$. Another representation is known to correspond to the critical square lattice Q states Potts model [1]. It involves a Q-dimensional representation V, and the relation to our parameter β is $Q = \beta^2$. The equivalence between 6 Vertex and Potts models can be proved by noting that a slight modification of our Temperley-Lieb vertex model (essentially by boundary terms) makes its partition function independent of the particular representation chosen [1].

A remarkable property of the Temperley-Lieb vertex model is that it can be reformulated as a dense loop model on the square lattice as follows.

The Temperley-Lieb algebra $TL_{N+1}(\beta)$ has a pictorial representation in which each generator is a rectangular domino with an upper and a lower line of points numbered $1, 2, \ldots, N+1$, connected by pairs through non-intersecting lines (strings). We have the following generators:

$1 =$

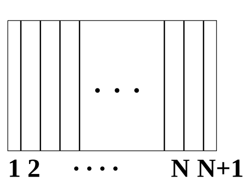

$U_i =$

(2.19)

A product of such generators is simply obtained by concatenation of the corresponding dominos. The relations of $TL_N(\beta)$ become transparent in the pictorial representation:

$U_i^2 \;=$ 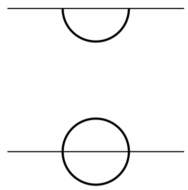

$U_i \, U_{i+1} \, U_i \;=$ 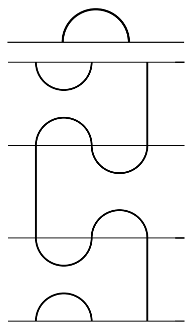

(2.20)

In particular we see that strings may be pulled (second relation) without altering the elements, and that loops may be replaced by a factor β (first relation). The most general elements of the algebra are linear combinations of the reduced products of generators, namely products in which we have pulled all strings and removed all loops.

As the identity is represented with only vertical strings, we may further simplify the notation and represent only the local part of the generators which is not the identity:

$U_i \;=$ 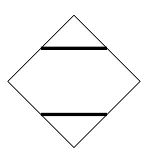 or

(2.21)

Another way of interpreting this is to view U as an operator acting (say from top to bottom) on a pair of strings by creating a bridge. As illustrated in (2.21), U_i corresponds to such an action on two consecutive strings, with positions i and $i+1$. Analogously, we may represent the identity acting on the same strings as

$1_i \;=$ 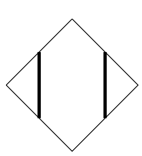

(2.22)

Consider now our Temperley-Lieb vertex model. The line of edges $V^{\otimes(N+1)}$ is now replaced by $N+1$ vertical strings. The operator $W_i(x)$ is a linear combination

$W_i(x) \;=$

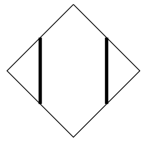

$+\frac{x}{z}$

(2.23)

where the strings have position i and $i+1$. Imposing periodic boundary conditions along the top and bottom ends of the strings, the partition function for a rectangle R' containing $N \times M$ vertices reads (we assume N and M to be even)

$$Z \;=\; \mathrm{Tr}\big((T_e T_o)^{M/2}\big) \tag{2.24}$$

where we have introduced even and odd transfer matrices

$$\begin{aligned} T_o &= W_1(x) W_3(x) \ldots W_{N-1}(x) \\ T_e &= W_2(x) W_4(x) \ldots W_N(x) \end{aligned} \tag{2.25}$$

The trace used in (2.24) is the standard Markov trace of $TL_{N+1}(\beta)$, defined on any reduced element by β^k, where k is the number of loops formed when we identify the top and bottom edges of the strings (e.g. $\mathrm{Tr}(1) = \beta^{N+1}$, $\mathrm{Tr}(U_i) = \beta^N$), and is extended to any element of the algebra by linearity. Comparing (2.24) with (2.5), we have in both cases simply rotated our view of the lattice by 45°, but the former rectangle (R) is rotated, while the new one is not, namely

$R =$

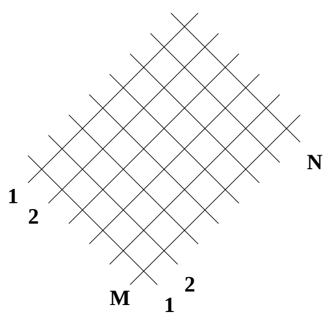

$R' =$

(2.26)

The expression (2.24) suggests the following interpretation of the model. We consider the dual R'^* of R', in which each vertex becomes a square face, rotated by 45°. Expanding the transfer matrices in (2.24) by using the expression (2.23), we can rewrite Z as a sum over the 2^{NM} face configurations on R'^* obtained by taking either the 1_i or the U_i term in each $W_i(x)$, and we still have to take the trace of this sum in $TL_{N+1}(\beta)$:

$$Z \;=\; \sum_{\text{face configurations}} a(x)^k \mathrm{Tr}(U_{i_1} U_{i_2} \ldots U_{i_k}) \tag{2.27}$$

But the trace of each term essentially produces a factor β^p, where p denotes the number of loops formed by the configuration of the faces of R'^*. Choosing x to be the isotropic point $x = z$, where $W_i = 1_i + U_i$, we have simply calculated the partition function of the dense loop model, whose configurations are the 2^{NM} face configurations obtained by taking either

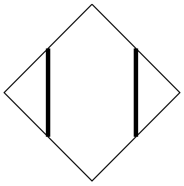

or

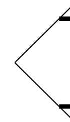

(2.28)

on each face of R'^*, and by attaching a weight β per loop.

3. The Bi-colored Dense Loop Model

In this section, we generalize the dense loop model by using the two-color Fuss-Catalan algebra recently introduced by Bisch and Jones [10].

3.1. The Fuss-Catalan Algebra

The two-color Fuss Catalan algebra $FC_{2N+2}(\alpha, \beta)$ is defined using the domino pictorial representation of previous section, but its elements must satisfy a further constraint. The dominos have $2N + 2$ top and bottom ends of strings, which are painted using two colors, say a and b, following the same pattern *abbaabbaabbaabba...* The latter ends either with a (N odd) or with a b (N even). The constraint is that only ends of the same color can be connected. In addition to the identity, which satisfies the constraint, this leads to the following generators:

$U_i^{(1)} =$ 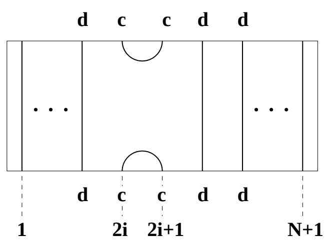

U_i

(3.1)

for $i = 1, 2, \ldots, N$. Note the positions at which these generators act: the position label i of U_i should be thought of as that of the center of the segment $2i, 2i + 1$, joining the corresponding string ends. When i is even, the central strings at positions $2i$ and $2i+1$ have color a. It is b when i is odd.

The pictorial representation translates into the following relations, where loops of color a (resp. b) receive a weight α (resp. β).

$$
\boxed{
\begin{aligned}
\big(U_i^{(1)}\big)^2 &= \begin{cases} \alpha U_i^{(1)} & \text{for } \ i \text{ even} \\ \beta U_i^{(1)} & \text{for } \ i \text{ odd} \end{cases} \\
\big(U_i^{(2)}\big)^2 &= \alpha\beta U_i^{(2)} \\
U_i^{(1)} U_i^{(2)} &= U_i^{(2)} U_i^{(1)} = \begin{cases} \alpha U_i^{(2)} & \text{for } \ i \text{ even} \\ \beta U_i^{(2)} & \text{for } \ i \text{ odd} \end{cases} \\
U_i^{(1)} U_{i+1}^{(1)} &= U_{i+1}^{(1)} U_i^{(1)} \\
U_i^{(1)} U_{i\pm1}^{(2)} U_i^{(1)} &= U_i^{(1)} U_{i\pm1}^{(1)} \\
U_i^{(2)} U_{i\pm1}^{(1)} U_i^{(2)} &= \begin{cases} \alpha U_i^{(2)} & \text{for } \ i \text{ even} \\ \beta U_i^{(2)} & \text{for } \ i \text{ odd} \end{cases} \\
U_i^{(2)} U_{i\pm1}^{(2)} U_i^{(2)} &= U_i^{(2)}
\end{aligned}
}
\tag{3.2}
$$

Note that $U^{(2)}$ is a generator of $TL_{N+1}(\alpha\beta)$. Note also that we may write more cubic relations, as consequences of (3.2), namely

$$
\begin{aligned}
U_i^{(1)} U_{i\pm1}^{(2)} U_i^{(2)} &= U_{i\pm1}^{(1)} U_i^{(2)} \\
U_i^{(2)} U_{i\pm1}^{(2)} U_i^{(1)} &= U_i^{(2)} U_{i\pm1}^{(1)}
\end{aligned}
\tag{3.3}
$$

3.2. The Yang-Baxter Solution

Let us look for solutions of the Yang-Baxter equation (2.6)(2.7)(2.8) in the form

$$
W_i(x) = 1_i + a(x) U_i^{(1)} + b(x) U_i^{(2)} \tag{3.4}
$$

Up to an interchange $i \leftrightarrow i+1$, we can always assume that i is even in (2.6). Using the relations (3.2), we have reexpressed (2.6) as a linear combination of reduced elements of $FC_{2N+2}(\alpha, \beta)$. Their coefficients must vanish, leading to the following equations (for simplicity, we have set $f(x)=f$, $f(xy)=f'$ and $f(y)=f''$ for $f=a,b$)

$$
\begin{aligned}
U_i^{(1)} &: \ a+a''+\alpha aa''-a'=0 \\
U_{i+1}^{(1)} &: \ a+a''+\beta aa''-a'=0 \\
U_i^{(2)} &: \ (1+\alpha a'')b+(1+\alpha a)b''+(\alpha\beta+\alpha a'+b')bb''-b'=0 \\
U_{i+1}^{(2)} &: \ (1+\beta a'')b+(1+\beta a)b''+(\alpha\beta+\beta a'+b')bb''-b'=0 \\
U_i^{(1)}U_{i+1}^{(2)}-U_i^{(2)}U_{i+1}^{(1)} &: \\
& \quad ab'-a'b-bb'a''-\beta ba'a''=0 \\
U_{i+1}^{(1)}U_i^{(2)}-U_{i+1}^{(2)}U_i^{(1)} &: \\
& \quad a'b''-a''b'+ab'b''+\alpha ba'a''=0
\end{aligned}
\tag{3.5}
$$

where we have indicated the corresponding element of $FC_{2N+2}(\alpha,\beta)$ in factor. Moreover, the normalization condition (2.7) yields, for even i (for simplicity, we have set $f(1/x)=\bar{f}$, for $f=a,b$)

$$
\begin{aligned}
a+\bar{a}+\alpha a\bar{a}=0 \\
(1+\alpha\bar{a})b+(1+\alpha a)\bar{b}+\alpha\beta b\bar{b}=0
\end{aligned}
\tag{3.6}
$$

As we are looking for non-trivial solutions, we want $a\neq 0$, hence from the first two lines of (3.5), we must have

$$
\alpha=\beta \tag{3.7}
$$

Expanding at first order in ϵ, with $y=e^{\epsilon}/x$, and using $a(1)=0$ from (2.8), we find the differential equation

$$
xa'(x)=a'(1)(1+\alpha a(x)) \tag{3.8}
$$

easily solved as $a(x)=(x^{\gamma}-1)/\alpha$, where we can set $\gamma=\alpha a'(1)$ to 1 without restrictions (by setting $x=e^{\gamma u}$ as before). This gives

$$
a(x)=\frac{x-1}{\alpha} \tag{3.9}
$$

Substituting this into the fifth equation of (3.5), we get

$$
(x-1-(y-1)b(x))b(xy)-y(xy-1)b(x)=0 \tag{3.10}
$$

Expanding to first order in ϵ, where $y=e^{\epsilon}$, we find the differential equation

$$
x(x-1)b'(x)-b(x)^2-(2x-1)b(x)=0 \tag{3.11}
$$

which may be recast into $\big(x(x-1)/b(x)\big)' = -1$, hence we have

$$b(x) = \frac{x(x-1)}{\mu - x} \tag{3.12}$$

for some integration constant μ. It is easy to see that μ is not determined by (3.10). The only equation left is the third line of (3.5), which yields

$$yb(x) + xb(y) + b(x)b(y)(\alpha^2 - 1 + xy) + b(xy)\big(b(x)b(y) - 1\big) = 0 \tag{3.13}$$

Substituting (3.12) into this, we finally get

$$\frac{xy(xy+1)(\alpha^2 - 1 - \mu)}{(\mu - x)(\mu - y)} = 0 \tag{3.14}$$

hence $\mu = \alpha^2 - 1$, and finally

$$b(x) = \frac{x(x-1)}{\alpha^2 - 1 - x} \tag{3.15}$$

To summarize, we have found a new hyperbolic solution of the Yang-Baxter equation of the form

$$\boxed{W_i(x) = 1_i + \frac{x-1}{\alpha} U_i^{(1)} + \frac{x(x-1)}{\alpha^2 - 1 - x} U_i^{(2)}} \tag{3.16}$$

where $U_i^{(1,2)}$ are the generators of the two-color Fuss-Catalan algebra $FC_{2N+2}(\alpha, \alpha)$, subject to (3.2) with $\alpha = \beta$. Note that we must take $\alpha^2 \neq 2$, in order for the condition (2.8) to hold. Moreover, if we insist on having positive Boltzmann weights, we must take $\alpha^2 > 2$ and the range of physical spectral parameters is given by

$$1 < x < \alpha^2 - 1 \tag{3.17}$$

3.3. The Loop Model

The solution (3.16) yields a new integrable model, which we now describe in terms of dense loops on the square lattice. First note that the pictorial representation (3.1) may be simplified by representing only the local part of the generators which is not the identity. This suggests to introduce the following face configurations

$1_i =$ 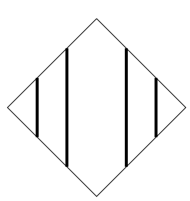 $U_i^{(1)}$

(3.18)

where the inner strings have color a if i is even, b if i is odd. Note that $\alpha = \beta$, hence we need not represent the strings with different colors, as eventually all the loops will receive the same weight α.

The partition function of the model on a rectangle with $M \times N$ faces is obtained by picking any of the three configurations of (3.18) on each face of the rectangle, and summing over all 3^{NM} possible configurations of the rectangle these generate. Each such configuration is weighed by a factor $a(x)^k b(x)^m$, where k and m denote the total numbers of faces of respectively the second and third types of (3.18). Imposing periodic boundary conditions on the top and bottom of the rectangle, the partition function is then obtained by taking the trace of the corresponding products of U_i's. This Markov trace is defined on any reduced element as $\alpha^p \beta^q$, where p and q denote respectively the total numbers of loops of color a and b, obtained by identifying the top and bottom of each string. The definition is extended to any element by linearity. As we have set $\alpha = \beta$, each loop configuration receives an extra weight α^p, where p is the total number of loops formed. To summarize, the partition function reads

$Z =$

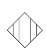 , 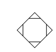

(3.19)

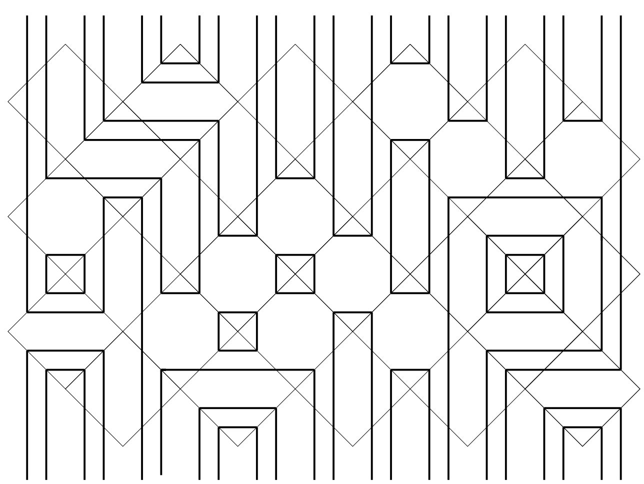

Fig. 1: A configuration of the two-color loop model. Each face is in one of the three face configurations of (3.18).

We have represented a typical configuration in Fig.1. Taking for x the isotropic value $x_* = \sqrt{\alpha^2 - 1}$, we have $b(x_*) = 1$ and $a(x_*) = (\sqrt{\alpha^2 - 1} - 1)/\alpha$. At this point, we simply have a model of loops, with partition function

$Z =$

 , 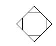

(3.20)

where k is the total number of faces of the second type in (3.18) and p the total number of loops.

Note that in this model the loops are fully packed and are colored with two colors, according to the pattern of the Fuss-Catalan algebra.

Note also the existence of a crossing symmetry for the Boltzmann weights (3.16), expressing the global covariance of the model under a rotation of 90°:

$$\bar{W}_i(x_*^2/x) = \frac{x_*^2 - x}{x(x-1)} \, W_i(x) \tag{3.21}$$

where $x_* = \sqrt{\alpha^2 - 1}$, and the bar stands for the effect of a rotation of 90°, namely $\bar{1}_i = U_i^{(2)}$, $\bar{U}_i^{(2)} = 1_i$, and $\bar{U}_i^{(1)} = U_i^{(1)}$. In particular, we have $\bar{W}_i(x_*) = W_i(x_*)$, hence the model (3.20) is invariant under rotation of 90°.

4. The Multi-colored Dense Loop Model

This section is an extension of the results of Sect.3 to the case of multi-colored loops. We find new hyperbolic solutions of the Yang-Baxter equation, based on the k-color Fuss-Catalan algebra.

4.1. Higher Fuss-Catalan Algebras

Higher Fuss-Catalan algebras have been introduced in [10], within the same type of pictorial representation as before, but now corresponding to painting the strings with k distinct colors $a_1, a_2, \ldots, a_k$, and attaching a weight α_j per loop of color a_j. These are the k-color Fuss-Catalan algebras, denoted by $FC_{k(N+1)}(\alpha_1, \alpha_2, \ldots, \alpha_k)$. Each domino has now $k(N+1)$ strings whose ends are painted following the pattern: $a_1 a_2 \ldots a_k a_k a_{k-1} \ldots a_2 a_1 a_1 a_2 \ldots$, both on the top and bottom ends. If N is odd the pattern ends with a_1, if N is even, with a_k. The constraint is now that a string may only connect points of the same color.

In analogy with Sect.3, we have found the k following types of generators for $m = 1, 2, \ldots, k$

$U_i^{(m)} =$ 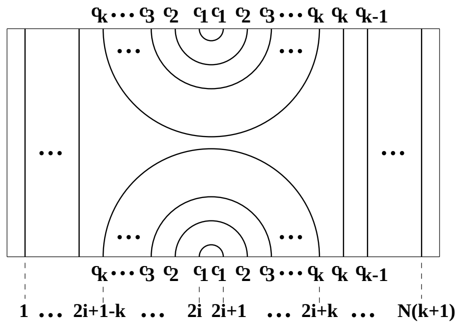

(4.1)

where $c_j = a_j$ if i is even, and $c_j = a_{k+1-j}$ if i is odd. These generators are all unnormalized projectors, and they satisfy the quadratic relations for $1 \leq m \leq p \leq k$

$$U_i^{(m)} U_i^{(p)} = U_i^{(p)} U_i^{(m)} = \rho_i(m) U_i^{(p)} \tag{4.2}$$

where

$$\rho_i(p) = \begin{cases} \alpha_1 \alpha_2 \ldots \alpha_p & \text{if } i \text{ even} \\ \alpha_k \alpha_{k-1} \ldots \alpha_{k+1-p} & \text{if } i \text{ odd} \end{cases} \tag{4.3}$$

The generators $U_i^{(m)}$ are local, hence

$$U_i^{(m)} U_j^{(p)} = U_j^{(p)} U_i^{(m)} \tag{4.4}$$

whenever $|i-j| > 1$, or when $|i-j| = 1$, and $m + p \leq k$.

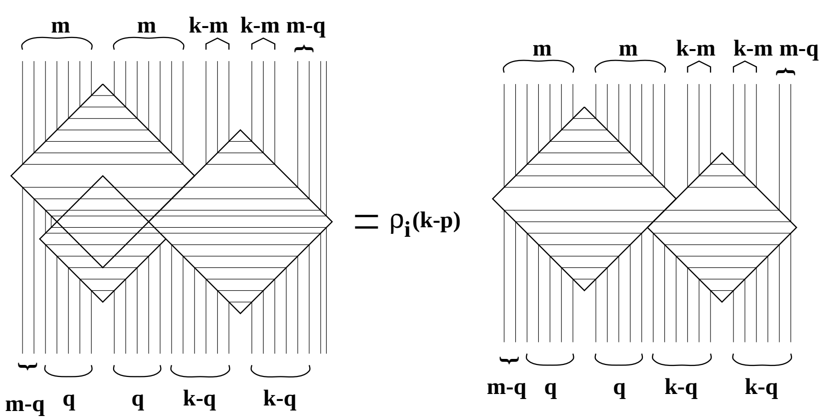

Fig. 2: The relation $U_i^{(m)} U_{i+1}^{(p)} U_i^{(q)} = \rho_i(k-p) U_i^{(m)} U_{i+1}^{(k-q)}$ for $m \geq q$. The generators are represented by squares of respective size m, p, q. The m and q boxes are first crushed into each other, by eliminating the $k-p$ loops created between them, and replacing them with the weight $\rho_i(k-p)$.

When these operators do not commute, it is easy to show that they always satisfy cubic relations generalizing (2.17), (3.2) and (3.3). These read

$$U_i^{(m)}U_{i\pm1}^{(p)}U_i^{(q)} = \rho_i(k-p)\begin{cases} U_i^{(m)}U_{i\pm1}^{(k-q)} & \text{if } m \geq q \\ U_{i\pm1}^{(k-m)}U_i^{(q)} & \text{if } m \leq q \end{cases} \tag{4.5}$$

with $\rho_i(p)$ as in (4.3). The first relation is explained in Fig.2. Note that the relations (4.2) and (4.5) are not independent. For instance, assume that $m \geq q$ in (4.5). Then multiplying the cubic relation by $U_i^{(r)}$ from the left, for $r > q$, and using the quadratic relations (4.2), we obtain the equation (4.5) with r substituted for m. This shows that we only need to write the relation for the smallest possible $m \geq q$, namely $m = q$, and that all the others will be consequences.

The k-color Fuss-Catalan algebra is therefore defined by the generators $1 \equiv U_i^{(0)}$ and $U_i^{(m)}$, $m = 1, 2, \ldots, k$ and $i = 1, 2, \ldots, N$, subject to the relations

$$\boxed{\begin{aligned} U_i^{(m)}U_i^{(p)} &= U_i^{(p)}U_i^{(m)} = \rho_i(m)U_i^{(p)} \\ U_i^{(m)}U_j^{(p)} &= U_j^{(p)}U_i^{(m)} \quad \text{if } |i-j|>1 \text{ or } j = i\pm1 \text{ and } m+p \leq k \\ U_i^{(m)}U_{i\pm1}^{(p)}U_i^{(m)} &= \rho_i(k-p)U_i^{(m)}U_{i\pm1}^{(k-m)} \quad \text{for } m+p > k \end{aligned}} \tag{4.6}$$

4.2. The Yang-Baxter Equation: I-Equations

Let us now look for a solution to the Yang-Baxter equation (2.6)(2.7)(2.8) in the form

$$W_i(x) = 1_i + \sum_{m=1}^{k} a_m(x)U_i^{(m)} \tag{4.7}$$

where $a_m(x)$ are some functions of x to be determined, and the $U_i^{(m)}$ are the generators of $FC_{k(N+1)}(\alpha_1, \ldots, \alpha_k)$.

As before, we simply have to expand (2.6) onto products of U's, which we must rearrange using the relations (4.2) and (4.5). Like in the case $k = 2$, let us restrict ourselves to even i, and denote by $\rho_m = \rho_i(m) = \alpha_1\alpha_2\ldots\alpha_m$, and by $\sigma_m = \rho_{i+1}(m) = \alpha_k\alpha_{k-1}\ldots\alpha_{k+1-m}$, with $\rho_0 = \sigma_0 = 1$. We list below the monomials in the U's and the corresponding vanishing coefficients (as before, we write f, f', f'' for $f(x), f(xy), f(y)$ respectively). We start with the first degree monomials:

$$\begin{aligned}
U_i^{(m)},\ 1 \leq m < k:\ & (\sum_{p=0}^{m-1} \rho_p a_p'')a_m + (\sum_{p=0}^{m-1} \rho_p a_p)a_m'' + \rho_m a_m a_m'' - a_m' = 0 \\
U_{i+1}^{(m)},\ 1 \leq m < k:\ & (\sum_{p=0}^{m-1} \sigma_p a_p'')a_m + (\sum_{p=0}^{m-1} \sigma_p a_p)a_m'' + \sigma_m a_m a_m'' - a_m' = 0 \\
U_i^{(k)} \qquad :\ & (\sum_{p=0}^{k-1} \rho_p a_p'')a_k + (\sum_{p=0}^{k-1} \rho_p a_p)a_k'' + (\sum_{p=0}^{k-1} \rho_p a_{k-p}')a_k a_k'' - a_k' = 0 \\
U_{i+1}^{(k)} \qquad :\ & (\sum_{p=0}^{k-1} \sigma_p a_p'')a_k + (\sum_{p=0}^{k-1} \sigma_p a_p)a_k'' + (\sum_{p=0}^{k-1} \sigma_p a_{k-p}')a_k a_k'' - a_k' = 0
\end{aligned} \tag{4.8}$$

where the extra terms for $m = k$ arise from the cubic relations $U_i^{(k)} U_{i+1}^{(k-p)} U_i^{(k)} = \rho_p U_i^{(k)}$, and $U_{i+1}^{(k)} U_i^{(k-p)} U_{i+1}^{(k)} = \sigma_p U_{i+1}^{(k)}$, for $p = 1, 2, \ldots, k$. The quadratic terms $U_i^{(m)} U_{i+1}^{(l)}$ or $U_{i+1}^{(m)} U_i^{(l)}$ are distinguished according to whether they commute ($m+l \leq k$) or not ($m+l > k$). Actually, the maximally commuting case $m + l = k$ must be treated separately. The commuting terms read:

$$\begin{aligned}
U_i^{(m)} U_{i+1}^{(l)}:\ & (\sum_{p=0}^{m-1} \rho_p a_p'')a_l' a_m'' + (\sum_{p=0}^{m-1} \rho_p a_p)a_m' a_l'' \\
& - (\sum_{p=0}^{l-1} \sigma_p a_p'')a_l a_m' - (\sum_{p=0}^{l-1} \sigma_p a_p)a_m' a_l'' = 0
\end{aligned} \tag{4.9}$$

for $m + l < k$. When $m + l = k$, we get some extra terms:

$$\begin{aligned}
& (\sum_{p=0}^{m-1} \rho_p a_p)a_{k-m}' a_m'' + (\sum_{p=0}^{m-1} \rho_p a_p'')a_{k-m}' a_m + (\sum_{p=0}^{m} \rho_p a_{k-p}')a_m a_m'' \\
& - (\sum_{p=0}^{k-m-1} \sigma_p a_p)a_{k-m}'' a_m' - (\sum_{p=0}^{k-m-1} \sigma_p a_p'')a_m' a_{k-m} - (\sum_{p=0}^{k-m} \sigma_p a_{k-p}')a_{k-m} a_{k-m}'' = 0
\end{aligned} \tag{4.10}$$

The non-commuting ones are

$$\begin{aligned}
U_i^{(m)}U_{i+1}^{(l)}:\ & (\sum_{p=0}^{k-l}\rho_p a_p'')a_m a_l' - (\sum_{p=0}^{k-m}\sigma_p a_p'')a_l a_m' \\
& + (\sum_{p=l+1}^{k}\rho_{k-p}a_p')a_m a_{k-l}'' - (\sum_{p=m+1}^{k}\sigma_{k-p}a_p')a_l a_{k-m}'' = 0 \\
U_{i+1}^{(m)}U_i^{(l)}:\ & (\sum_{p=0}^{k-l}\sigma_p a_p)a_m'' a_l' - (\sum_{p=0}^{k-m}\rho_p a_p)a_l'' a_m' \\
& + (\sum_{p=l+1}^{k}\sigma_{k-p}a_p')a_m'' a_{k-l} - (\sum_{p=m+1}^{k}\rho_{k-p}a_p')a_l'' a_{k-m} = 0
\end{aligned} \tag{4.11}$$

for $m + l > k$.

4.3. The Yang-Baxter Equation: II-Solutions

The first two equations of (4.8) have non-trivial solutions with $a_m \neq 0$ only if both are the same, namely $\sigma_p = \rho_p$ for $p = 1, 2, \ldots, k$, which implies that

$$\alpha_m = \alpha_{k+1-m} \quad \text{for} \;\; 1 \leq m \leq k \tag{4.12}$$

This implies also that the two equations of (4.11) are equivalent. Note that the first equation of (4.8) for $m = 1$ coincides with the first line of (3.5), with $\alpha = \beta$ replaced by $\alpha_1 = \alpha_k$. Hence we have the solution

$$a_1(x) = \frac{x^{r_1} - 1}{\alpha_1} \tag{4.13}$$

where r_1 can be set to 1 as usual (we will however keep r_1 in the formulas, for the sake of uniformity). For $m = 2$, we have

$$(1 + \alpha_1 a_1(y))a_2(x) + (1 + \alpha_1 a_1(x))a_2(y) + \alpha_1\alpha_2 a_2(x)a_2(y) - a_2(xy) = 0 \tag{4.14}$$

Writing $a_2(x) = x^{r_1} m_2(x)$, and using the value (4.13), we find

$$m_2(x) + m_2(y) + \alpha_1\alpha_2 m_2(x)m_2(y) - m_2(xy) = 0 \tag{4.15}$$

This is again the first equation of (3.5), with the substitution $\alpha \to \alpha_1\alpha_2$. We deduce the solution $m_2(x) = (x^{r_2} - 1)/(\alpha_1\alpha_2)$, where r_2 is an arbitrary nonzero number, hence

$$a_2(x) = \frac{1}{\rho_2} x^{r_1}(x^{r_2} - 1) \tag{4.16}$$

Proceeding by induction, assume $a_p = x^{r_1+r_2+\ldots+r_{p-1}}(x^{r_p}-1)/\rho_p$, for all $p \leq q-1$, and some non-vanishing numbers $r_1 = 1, r_2, \ldots, r_{q-1}$. Then, setting $a_q = x^{r_1+r_2+\ldots+r_{q-1}} m_q(x)$, and noting that

$$\sum_{p=0}^{q-1} \rho_p a_p(x) = x^{r_1+r_2+\ldots+r_{q-1}} \tag{4.17}$$

the equation for m_q is nothing but again the first equation of (3.5), with $\alpha \to \rho_q$. We therefore get $m_q = (x^{r_q}-1)/\rho_q$ for some non-vanishing number r_q, and

$$a_m(x) = \frac{1}{\rho_m} x^{r_1+r_2+\ldots+r_{m-1}}(x^{r_m}-1) \tag{4.18}$$

for all $m = 1, 2, \ldots, k-1$, and $r_i \neq 0$, $i = 1, 2, \ldots, k-1$.

Let us now turn to the commuting second order term equations (4.9). The solutions (4.18) satisfy them automatically. Indeed, using (4.12) and (4.17), (4.9) read

$$\begin{aligned}
&x^{r_1+r_2+\ldots+r_{m-1}} a_l' a_m'' + y^{r_1+r_2+\ldots+r_{m-1}} a_m a_l' + \rho_m a_m a_l' a_m'' \\
&- x^{r_1+r_2+\ldots+r_{l-1}} a_m' a_l'' - y^{r_1+r_2+\ldots+r_{l-1}} a_l a_m' - \rho_l a_l a_m' a_l'' \\
&= \frac{1}{\rho_m \rho_l} (xy)^{r_1+\ldots+r_{m-1}+r_1+\ldots+r_{l-1}} \Big(((xy)^{r_l}-1)(x^{r_m}-1+y^{r_m}-1) \\
&- ((xy)^{r_m}-1)(x^{r_l}-1+y^{r_l}-1) + ((xy)^{r_l}-1)(x^{r_m}-1)(y^{r_m}-1) \\
&\qquad - ((xy)^{r_m}-1)(x^{r_l}-1)(y^{r_l}-1) \Big) = 0
\end{aligned} \tag{4.19}$$

where we have substituted the values (4.18) (note that $m + l \leq k$ and $m, l \geq 1$, hence $m, l \leq k-1$ and (4.18) applies).

Let us now use the highest non-trivial of the non-commuting equations (4.11), for $m = k$ and $l = k-1$ (for $m = l = k$ the coefficient is identically zero). This gives

$$(a_{k-1}(x) - a_k(x) a_1(y)) a_k(xy) = y a_k(x) a_{k-1}(xy) \tag{4.20}$$

Introducing the ratio

$$\varphi_1(x) = x \frac{a_{k-1}(x)}{a_k(x)} \tag{4.21}$$

this becomes

$$\varphi_1(xy) - \varphi_1(x) = -\frac{x(y-1)}{\rho_1} \tag{4.22}$$

Setting $y = e^\epsilon$ and expanding to first order in ϵ, we get $\varphi_1'(x) = -1/\rho_1$, easily integrated into

$$\varphi_1(x) = \frac{\mu - x}{\rho_1} \tag{4.23}$$

for some integration constant μ. From the definition (4.21), we deduce

$$a_k(x) = \frac{\rho_1}{\rho_{k-1}} x^{r_1+r_2+\ldots+r_{k-2}+1} \frac{x^{r_{k-1}}-1}{\mu - x} \tag{4.24}$$

Note that $\mu \neq 1$ in order for the initial condition $a_k(1) = 0$ to be satisfied. It is easy to check that (4.23) satisfies the initial equation (4.22) trivially, for any μ.

We can now substitute the forms (4.18)(4.24) into the remaining equations, to further fix the parameters. Let us now use (4.11) for $m = k$ and $l = k-2$. The equation reads

$$\frac{a_{k-2}(x)}{a_k(x)} = a_2(y)(1+\rho_1 \frac{a_{k-1}(xy)}{a_k(xy)} + (1+\rho_1 a_1(y) + \rho_2 a_2(y)) \frac{a_{k-2}(xy)}{a_k(xy)} \tag{4.25}$$

Using the value (4.21), the identity $1+\rho_1 a_1(y)+\rho_2 a_2(y) = y^{r_1+r_2}$ from (4.17), and setting $\varphi_2(x) = x^{r_1+r_2} a_{k-2}(x)/a_k(x)$, we get

$$\varphi_2(xy) - \varphi_2(x) = -\frac{\mu}{\rho_2} x^{r_2}(y^{r_2}-1) \tag{4.26}$$

Setting $y = e^{\epsilon}$ and expanding to first order in ϵ, we find the differential equation

$$\varphi_2'(x) = -\frac{\mu}{\rho_2} r_2 x^{r_2-1} \tag{4.27}$$

easily integrated as

$$\varphi_2(x) = \frac{\mu}{\rho_2}(\mu^{r_2} - x^{r_2}) \tag{4.28}$$

as $\varphi_2(x)$ vanishes at $x = \mu$. We may now proceed by induction. Assume

$$\varphi_p(x) = \frac{1}{\rho_p} \mu^{r_1+r_2+\ldots+r_{p-1}}(\mu^{r_p} - x^{r_p}) \tag{4.29}$$

for all $p \leq q-1$. Then writing the equation (4.11) for $m = k$ and $l = k-q$ and dividing it by $a_k a_k'$, we get

$$\begin{aligned} \varphi_q(xy) - \varphi_q(x) &= -x^{r_1+\ldots+r_q} a_q''\big(1 + \frac{\rho_1}{xy}\varphi_1(xy) + \ldots + \frac{\rho_{q-1}}{(xy)^{r_1+\ldots+r_{q-1}}}\varphi_{q-1}(xy)\big) \\ &= -\frac{1}{\rho_q}\mu^{r_1+\ldots+r_q} x^{r_p}(y^{r_p}-1) \end{aligned} \tag{4.30}$$

where we have used the induction hypothesis (4.29). Setting $y = e^{\epsilon}$, and expanding to first order in ϵ, we get a differential equation, easily integrated as

$$\varphi_q = \frac{1}{\rho_q} \mu^{r_1+r_2+\ldots+r_{q-1}}(\mu^{r_q} - x^{r_q}) \tag{4.31}$$

which therefore holds for all $q = 1, 2, \ldots, k-1$. Note the following remarkable property of this solution, namely that

$$1 + \frac{\rho_1}{x^{r_1}}\varphi_1(x) + \frac{\rho_2}{x^{r_1+r_2}}\varphi_2(x) + \ldots + \frac{\rho_m}{x^{r_1+\ldots+r_m}}\varphi_m(x) = \big(\frac{\mu}{x}\big)^{r_1+\ldots+r_m} \tag{4.32}$$

This will be used extensively later.

We have now two values for the ratios (4.21). One is (4.31), the other is obtained by substituting (4.18) into the definition (4.31). Both agree if

$$\frac{1}{\rho_q}\mu^{r_1+r_2+\ldots+r_{q-1}}(\mu^{r_q} - x^{r_q}) = \frac{\rho_{k-1}}{\rho_1\rho_{k-q}}\frac{x^{r_1+\ldots+r_q}(x^{r_{k-q}}-1)(\mu - x)}{x^{r_{k-q}+\ldots+r_{k-2}}(x^{r_{k-1}}-1)} \tag{4.33}$$

for all $q = 1, 2, \ldots, k-1$. The simplest way to analyze these equations is to take the ratio of two consecutive ones, leading to

$$x^{r_{k-q}}(x^{r_q} - \mu^{r_q})(x^{r_{k-q-1}} - 1) = \frac{\alpha_q^2}{\mu^{r_{q-1}}}x^{r_q}(x^{r_{q-1}} - \mu^{r_{q-1}})(x^{r_{k-q}} - 1) \tag{4.34}$$

for $q = 2, 3, \ldots, k-1$. The r's are all non-zero real numbers. By inspection of the 16 possibilities for the signs of $(r_{q-1}, r_q, r_{k-q-1}, r_{k-q})$, we see that only two do not lead to contradictions, namely

(i) $r_{q-1} = r_q = r_{k-q} = r_{k+1-q}$, and $\mu = \alpha_q^2$.

(ii) $r_{q-1} = -r_q$, $r_{k-q} = -r_{k+1-q}$, and $\alpha_q^2 = 1$.

Note that in both cases we have

$$\alpha_q^2 = \mu^{(r_q + r_{q-1})/2} \tag{4.35}$$

We will discuss these solutions later, let us first write all remaining equations.

Let us turn to (4.10). Dividing it by a'_k, and using (4.31), it reads

$$\begin{aligned}
&\big(1 + \frac{\rho_1}{xy}\varphi_1(xy) + \ldots + \frac{\rho_{m-1}}{(xy)^{r_1+\ldots+r_{m-1}}}\varphi_{m-1}(xy)\big)a_m a''_m \\
&- \big(1 + \frac{\rho_1}{xy}\varphi_1(xy) + \ldots + \frac{\rho_{k-m-1}}{(xy)^{r_1+\ldots+r_{k-m-1}}}\varphi_{k-m-1}(xy)\big)a_{k-m}a''_{k-m} \\
&= \frac{1}{\rho_m^2}\mu^{r_1+\ldots+r_{m-1}}(x^{r_m}-1)(y^{r_m}-1) \\
&- \frac{1}{\rho_{k-m}^2}\mu^{r_1+\ldots+r_{k-m-1}}(x^{r_{k-m}}-1)(y^{r_{k-m}}-1) = 0
\end{aligned} \tag{4.36}$$

where we have used the identity (4.32). This must hold for all x, y, hence

$$r_m = r_{k-m} \tag{4.37}$$

for $m = 1, 2, \dots, k-1$. In particular, we learn that $r_{k-1} = r_1 = 1$. The coefficients must also agree, hence

$$\left(\frac{\alpha_1 \dots \alpha_m}{\alpha_1 \dots \alpha_{k-m}}\right)^2 = \frac{\mu^{r_1+\dots+r_m}}{\mu^{r_1+\dots+r_{k-m}}} \tag{4.38}$$

This identity is a direct consequence of (4.35).

To proceed, let us check the other non-commuting second degree terms (4.11), namely with $m + l > k$, $m, l < k$. Let us take $m = k - p$ and $l = k - s$ in (4.11), mutliply it by $x^{r_1+\dots+r_p+r_1+\dots+r_s}$, and use (4.32) to get

$$\begin{aligned} &\varphi_s(x)\varphi_p(xy) - \varphi_s(x)\varphi_p(xy) = \\ &\big(\frac{\mu x}{xy}\big)^{r_1+\dots+r_{s-1}} x^{r_s} \varphi_p(x) a_s(xy) - \big(\frac{\mu x}{xy}\big)^{r_1+\dots+r_{p-1}} x^{r_p} \varphi_s(x) a_p(xy) \end{aligned} \tag{4.39}$$

This is easily checked, by substituting the solution (4.31), and using (4.38).

Finally, let us write the first degree equation (4.8) for $m = k$, using both (4.17) and (4.32):

$$\begin{aligned} a_k(x)a_k(xy)a_k(y)\big(\frac{\mu}{xy}\big)^{r_1+\dots+r_{k-1}} + \rho_k a_k(x)a_k(y) + y^{r_1+\dots+r_{k-1}} a_k(x) \\ - x^{r_1+\dots+r_{k-1}} a_k(y) - a_k(xy) = 0 \end{aligned} \tag{4.40}$$

Substituting the value (4.24), we get after some algebra

$$\begin{aligned} &\frac{(xy)^{1+r_1+\dots+r_{k-2}} \rho_1 (x-1)(xy-1)(y-1)}{\rho_{k-1}(\mu - x)(\mu - xy)(\mu - y)} \times \\ &\times \Big((xy-1)\big(\mu(x-1)(y-1) - (\mu - x)(\mu - y)\big) \\ &+ xy(\mu - xy)\big(\alpha_1^2 (x-1)(y-1) + (x-1)(\mu - y) + (y-1)(\mu - x)\big)\Big) \end{aligned} \tag{4.41}$$

where we have used (4.38) for $m = 1$, $\rho_1 \rho_k / \rho_{k-1} = \alpha_1^2$, and the values $r_{k-1} = r_1 = 1$. The last factor can be rearranged into

$$\begin{aligned} (1-\mu)(xy-1)(\mu - xy) + (\mu - xy)\big((\mu - 1)(xy - 1) + (1 + \mu - \alpha_1^2)(x+y)\big) \\ = (\mu - xy)(1 + \mu - \alpha_1^2)(x+y) \end{aligned} \tag{4.42}$$

This vanishes for all x, y if

$$\mu = \alpha_1^2 - 1 \tag{4.43}$$

To summarize, we have found all solutions $a_1(x), a_2(x), \ldots, a_k(x)$ to all the equations implied by (2.6)(2.7)(2.8). These solutions read (4.18)(4.24), with integers $r_i \in \{\pm 1\}$, loop weights $\alpha_1, \alpha_2, \ldots, \alpha_k$, and a parameter μ such that

$$\begin{aligned}
r_1 = r_{k-1} &= 1 \\
\text{and} &\begin{cases} \text{either} & r_{q-1} = r_q = r_{k-q} = r_{k+1-q} \\ \text{or} & r_{q-1} = -r_q = -r_{k-q} = r_{k+1-q} \end{cases} \\
\mu^{\frac{r_{q-1}+r_q}{2}} &= \alpha_q^2 \\
\mu &= \alpha_1^2 - 1 \\
\alpha_q &= \alpha_{k+1-q}
\end{aligned} \tag{4.44}$$

Let us start from the fundamental solution $r_1 = r_2 = \ldots = r_{k-1} = 1$, which has $\mu = \alpha_1^2 - 1 = \alpha_2^2 = \alpha_3^2 = \ldots = \alpha_{k-1}^2$ i.e.

$$\alpha_2 = \alpha_3 = \ldots = \alpha_{k-1} = \sqrt{\alpha_1^2 - 1} \tag{4.45}$$

if all α's are positive, and

$$\boxed{\begin{aligned}
a_q(x) &= \frac{x^{q-1}}{\alpha_1(\alpha_1^2-1)^{\frac{q-1}{2}}}(x-1) \quad q = 1, 2, \ldots, k-1 \\
a_k(x) &= \frac{x^{k-1}}{(\alpha_1^2-1)^{\frac{k}{2}-1}} \frac{x-1}{\alpha_1^2 - 1 - x}
\end{aligned}} \tag{4.46}$$

This solution generalizes (3.16) to the case of k-color Fuss-Catalan algebras. Note that we have positive Boltzmann weights only if $\alpha^2 > 2$, and

$$1 < x < \alpha^2 - 1 \tag{4.47}$$

The other solutions can be obtained by elementary "q-excitations" in which we reverse all values of r_i for $i = q, q+1, \ldots, k-q$. Indeed, these excitations must be symmetric, as they impose that some $\alpha_q = \alpha_{k+1-q}$ change its value from μ to 1 or vice versa. We can apply these excitations at any $q = 2, 3, \ldots, \ell$, where $\ell = [(k+1)/2]$, hence a total of $2^{\ell-1}$ solutions, of the form $r_1 = \ldots = r_{i_1-1} = 1$, $r_{i_1} = \ldots = r_{i_2-1} = -1$, ... ,

$r_{i_s} = \ldots = r_\ell = (-1)^s$, corresponding to s such excitations, $s = 0, 1, \ldots, \ell - 1$. The simplest such solution occurs for $k = 4$, where we have a total of two solutions

$$\begin{aligned}
&(1)\ \text{fundamental}: \ r_1 = r_2 = r_3 = 1 \qquad \alpha_1 = \alpha_4 = \alpha, \quad \alpha_2 = \alpha_3 = \alpha^2 - 1 \\
&\quad W_i^{(1)}(x) = 1_i + \frac{x-1}{\alpha} U_i^{(1)} + \frac{x(x-1)}{\alpha\sqrt{\alpha^2-1}} U_i^{(2)} \\
&\qquad\qquad + \frac{x^2(x-1)}{\alpha(\alpha^2-1)} U_i^{(3)} + \frac{x^3(x-1)}{(\alpha^2-1)(\alpha^2-1-x)} U_i^{(4)} \\
&(2)\ \text{excited}: \ r_1 = r_3 = 1, \ r_2 = -1 \qquad \alpha_1 = \alpha_4 = \alpha, \quad \alpha_2 = \alpha_3 = 1 \\
&\quad W_i^{(2)}(x) = 1_i + \frac{x-1}{\alpha} U_i^{(1)} - \frac{(x-1)}{\alpha} U_i^{(2)} \\
&\qquad\qquad + \frac{(x-1)}{\alpha} U_i^{(3)} + \frac{x(x-1)}{(\alpha^2-1-x)} U_i^{(4)}
\end{aligned} \tag{4.48}$$

Note that at the self-dual point $x = \sqrt{\alpha^2 - 1}$ these solutions read

$$\begin{aligned}
W_i^{(1)} &= 1_i + \frac{\sqrt{\alpha^2-1}-1}{\alpha} \big(U_i^{(1)} + U_i^{(2)} + U_i^{(3)}\big) + U_i^{(4)} \\
W_i^{(2)} &= 1_i + \frac{\sqrt{\alpha^2-1}-1}{\alpha} \big(U_i^{(1)} - U_i^{(2)} + U_i^{(3)}\big) + U_i^{(4)}
\end{aligned} \tag{4.49}$$

where they not only differ by the sign in front of $U_i^{(2)}$ but also by $\alpha_2 = \alpha_3 = \sqrt{\alpha^2 - 1}$ in the case (1) and $\alpha_2 = \alpha_3 = 1$ in the case (2).

4.4. The Loop Models

In this section, we concentrate on the "fundamental" solution (4.46) found above, with $\alpha_2 = \ldots = \alpha_{k-1} = \sqrt{\alpha_1^2 - 1}$, and

$$\boxed{W_i(x) = 1_i + \sum_{q=1}^{k-1} \frac{x^{q-1}}{(\alpha_1^2-1)^{\frac{q-1}{2}}} \frac{x-1}{\alpha_1} U_i^{(q)} + \frac{x^{k-1}}{(\alpha_1^2-1)^{\frac{k}{2}-1}} \frac{x-1}{\alpha_1^2-1-x} U_i^{(k)}} \tag{4.50}$$

Let us represent the projectors (4.1) as "face operators" generalizing (3.18), namely

$U_i^{(m)} =$ 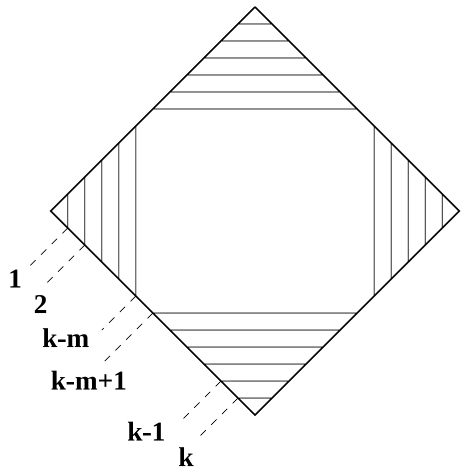

(4.51)

This gives rise to the following partition function for the mutlicolored dense loop model, generalizing (3.19), with loops of colors $1, 2, \ldots, k$:

$$Z = \sum_{\text{face configs}} \alpha_1^{L_1+L_k} (\alpha_1^2 - 1)^{\frac{1}{2}(L_2+\ldots+L_{k-1})} \prod_{m=1}^{k} a_m(x)^{N_m} \tag{4.52}$$

where L_i is the number of loops of color i, and N_m the number of occurrences of the face corresponding to $U_i^{(m)}$.

As before, the models obeys a crossing symmetry relation, expressing the covariance of the Boltzmann weights under a rotation of 90° of the faces

$$\bar{W}_i(x_*^2/x) = x_*^{k-2} \frac{x_*^2 - x}{x^{k-1}(x-1)} \, W_i(x) \tag{4.53}$$

with $x_* = \sqrt{\alpha_1^2 - 1}$, and where the bar stands for the rotation of 90°, with $\bar{U}_i^{(m)} = U_i^{(k-m)}$, for $m = 0, 1, \ldots, k$ (we define $U^{(0)} = 1$). The rotationally invariant weights are $W_i(x_*)$. In the corresponding model, the loops are weighted as in (4.52), whereas $a_1(x_*) = a_2(x_*) = \ldots = a_{k-1}(x_*) = (\sqrt{\alpha_1^2 - 1} - 1)/\alpha_1$, and $a_k(x_*) = 1$.

5. Discussion and Conclusion

5.1. Coloring Algebras

The Fuss-Catalan algebras can also be viewed as subalgebras of $TL_n(\alpha_1) \otimes TL_n(\alpha_2) \otimes \ldots \otimes TL_n(\alpha_k)$ (with generators $u_i^{(m)} \in TL_n(\alpha_m)$), by expressing their generators as

$$U_i^{(m)} = \begin{cases} 1 \otimes 1 \otimes \ldots \otimes 1 \otimes u_i^{(k-m+1)} \otimes u_i^{(k-m+2)} \otimes \ldots \otimes u_i^{(k)} & \text{if } i \text{ odd} \\ u_i^{(1)} \otimes u_i^{(2)} \otimes \ldots \otimes u_i^{(m)} \otimes 1 \otimes 1 \otimes \ldots \ldots \otimes 1 & \text{if } i \text{ even} \end{cases} \tag{5.1}$$

where there are exactly k factors in both tensor products. For $k = 2$ this reads

$$1_i = 1_a \otimes 1_b \qquad U_i^{(1)} = \begin{cases} 1_a \otimes U_b & \text{if } i \text{ odd} \\ U_a \otimes 1_b & \text{if } i \text{ even} \end{cases} \qquad U_i^{(2)} = U_a \otimes U_b \tag{5.2}$$

where the subscripts a, b refer to the corresponding algebras $TL_n(\alpha), TL_n(\beta)$.

In principle, we could use this as a recipee for "coloring" any algebra. In particular, let us color the Hecke algebra $H_n(\beta)$, by introducing generators $V_i^{(m)}$, in the same way as in (5.1), but using the generators of the Hecke algebras $H_n(\alpha_m)$ instead of the $u^{(m)}$. Looking for a solution of the Yang-Baxter system (2.6)(2.7)(2.8) of the form

$$W_i(x) = 1 + \sum_{m=1}^{k} a_m(x) V_i^{(m)} \tag{5.3}$$

we have found that there is no non-trivial solution unless the initial algebras actually obey the Temperley-Lieb relations (2.17). Hence, the coloring process is particular to Temperley-Lieb, in the sense that, only in that case, we get new solutions to the Yang-Baxter equation.

5.2. ADE Colored Models

The Boltzmann weights (4.50) of the colored loop models are related to Temperley-Lieb algebra generators through (5.1). An explicit model is obtained by choosing a particular representation of these Temperley-Lieb algebras, to build a representation of the corresponding Fuss-Catalan algebra. For instance, when $k = 2$, using the 4×4 representation (2.18) for all the Temperley-Lieb algebras $TL_n(\alpha_m)$, $m = 1, 2$, we get a 16×16 matrix representation for $W_i(x)$, which reads in 4×4 block-form

$$\begin{aligned} W_{\text{odd}} &= \begin{pmatrix} 1 + aU & 0 & 0 & 0 \\ 0 & 1 + (a + bz)U & bU & 0 \\ 0 & bU & 1 + (a + b/z)U & 0 \\ 0 & 0 & 0 & 1 + aU \end{pmatrix} \\ W_{\text{even}} &= \begin{pmatrix} 1 & 0 & 0 & 0 \\ 0 & (1 + az)1 + bzU & a1 + bU & 0 \\ 0 & a1 + bU & (1 + a/z)1 + b/zU & 0 \\ 0 & 0 & 0 & 1 \end{pmatrix} \end{aligned} \tag{5.4}$$

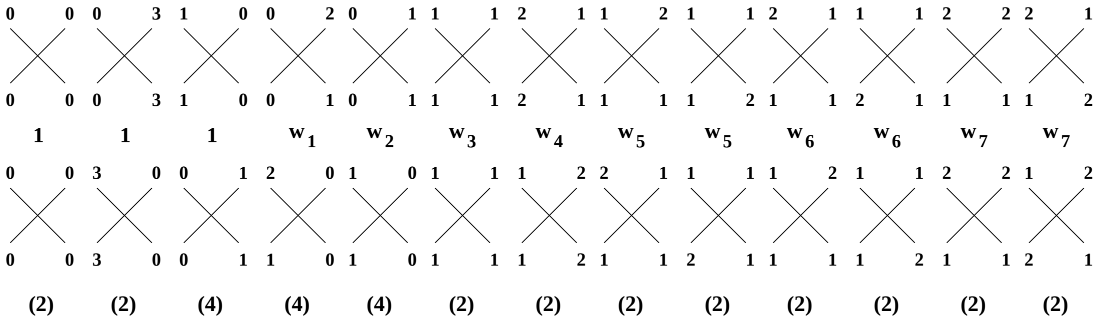

Fig. 3: The inhomogeneous 32 vertex model corresponding to the two-color Fuss-Catalan solution to the Yang-Baxter equation. We have represented in the first (resp. second) line the non-vanishing odd (resp. even) vertices, together with their Boltzmann weights: $w_1 = a$, $w_2 = 1+az$, $w_3 = 1+az+bz^2$, $w_4 = 1 + az + b$, $w_5 = a + bz$, $w_6 = bz$, $w_7 = b$, with a and b as in (3.9) and (3.15). To actually get all the vertices (their total numbers are indicated in parentheses), we must apply the two following transformations: (i) under $0 \leftrightarrow 3$, the Boltzmann weights are unchanged; (ii) under $1 \leftrightarrow 2$, we must also change $z \to 1/z$. Note that the second line of vertices is obtained from the first by interchanging the two spaces over which the operator W acts, in agreement with (5.2).

with U as in (2.18), and 1 the 4×4 identity matrix.

We may therefore view the two-color model as an inhomogeneous 32-Vertex model on the square lattice, the vertices being the non-zero entries in (5.4). These correspond naturally to edge states taking four possible values $0, 1, 2, 3$ (see Fig.3).

Our result however is independent of the particular choices of the representations of the Temperley-Lieb algebras. In particular, we could take different representations for the various factors $TL_n(\alpha_m)$. For any connected non-oriented graph Γ with adjacency matrix entries $G_{i,j} \in \{0, 1\}$ and $G_{i,i} = 0$, and each eigenvector of G with non-vanishing entries S_i and eigenvalue β, one has the following representation of $TL_n(\beta)$

1 (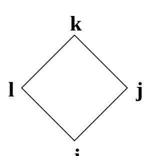

) $= \delta_{i,k}$, (5.5)

where i, j, k, l are now vertex variables on the square lattice, taking their values among the vertices of the target graph Γ, and such that any two neighboring vertices of the lattice have values linked by an edge on Γ. It has been shown that if $G = A, D, E$, one of the simply-laced Dynkin diagrams, this representation leads through (2.15) to the Boltzmann weights of some of the A, D, E minimal models (with largest eigenvalue $\beta = 2\cos(\pi/m)$,

$m = 2, 3, 4, ...$) [12][14] (dilute vertex models must be considered as well to exhaust all the list, see [13][14]), whereas the extended Dynkin diagrams $\hat{A}, \hat{D}, \hat{E}$ (with largest eigenvalue $\beta = 2$) lead to the free bosonic theory compactified on circles of specific radii.

In the k-colored case, our "fundamental" Boltzmann weights (4.50) for arbitrary choices of A, D, E representations in each factor give a number of new vertex models, with target space a tensor product of k simply-laced Dynkin diagrams. In the unitary case, where all Boltzmann weights are positive, we must restrict the choice of eigenvector to the Perron-Frobenius one, namely corresponding to the largest eigenvalue β. In that case, the target space takes the form $G_1 \times G_2 \times \ldots \times G_k$, where $G_i \in \{A, D, E\}$, and where the maximum eigenvalue of G_1, G_k is $\alpha_1 = 2\cos(\pi/m_1)$, and that of $G_2, G_3, \ldots, G_{k-1}$ is $\sqrt{\alpha_1^2 - 1} = 2\cos(\pi/m_2)$, where we have identified the Coxeter numbers m_1, m_2 of the Dynkin diagrams. This is actually only possible for the following values of m_i: $(m_1, m_2) = (3, 2); (6, 4)$, hence only for $(\alpha_1, \alpha_2) = (1, 0); (\sqrt{3}, \sqrt{2})$ (only the last case will have positive Boltzmann weights, when (4.47) holds). This leaves us with only the Dynkin diagrams of A_3, A_5 and D_4, with respective Coxeter number 4, 6 and 6.

Even in general, the condition that both α_1 and $\sqrt{\alpha_1^2 - 1}$ be eigenvalues of Dynkin diagrams is very restrictive, and we are left only with $(\alpha_1, \alpha_2) = (1, 0); (\sqrt{3}, \sqrt{2})$. These can appear as (non-necessarily Perron-Frobenius) eigenvalues of a number of Dynkin diagrams.

We can also consider the case where we take ADE representations for say $TL_n(\alpha_1)$ and $TL_n(\alpha_k)$, and a 6 vertex representation for the other factors $TL_n(\alpha_i)$, $i = 2, 3, ..., k-1$. In that case, any ADE is allowed, and if $\alpha_1 = 2\cos(\pi/m)$, then $\alpha_2 = \sqrt{4\cos^2(\pi/m) - 1}$ for $m = 2, 3, 5, 6, ...$, where again we have excluded $m = 4$ as it leads to $\mu = 1$. Conversely, we may take any ADE representation for $TL_n(\alpha_i)$, $i = 2, 3, ..., k-1$, and a 6 vertex representation for $TL_n(\alpha_1)$ and $TL_n(\alpha_k)$. In the latter case, we have $\alpha_2 = 2\cos(\pi/m)$, and $\alpha_1 = \sqrt{4\cos^2(\pi/m) + 1}$, $m = 3, 4, 5, ...$

Finally, we could also take $\hat{A}\hat{D}\hat{E}$ representations say for $TL_n(\alpha_1)$ and $TL_n(\alpha_k)$, when $\alpha_1 = \alpha_k = 2$, and then either A_5 or D_6 representations for $TL_n(\alpha_m)$, $m = 2, 3, ..., k-1$, with all $\alpha_m = \sqrt{3}$. Conversely, we may take $\hat{A}\hat{D}\hat{E}$ representations for $TL_n(\alpha_m)$, $m = 2, 3, ..., k-1$, with all $\alpha_m = 2$, and a 6 vertex representation for $TL_n(\alpha_1)$ and $TL_n(\alpha_k)$, with $\alpha_1 = \alpha_k = \sqrt{5}$.

Allowing for excited solutions with some negative r_i's, this gives the possibility of choosing an A_2 representation for the $TL_n(\alpha_i)$ factors with $\alpha_i = 1 = 2\cos(\pi/3)$ (namely such that $r_i = -r_{i-1}$).

5.3. *Rational Limit*

The Boltzmann weights (4.50) admit a rational limit, obtained by setting $x = e^{\epsilon u}$ and $\alpha_1^2 - 1 = e^{\epsilon}$, and letting $\epsilon \to 0$. We immediately get

$$W_i^{rat}(u) = 1_i + \frac{u}{1-u} U_i^{(k)} \tag{5.6}$$

But, thanks to (4.6), the $U_i^{(k)}$ generate a Temperley-Lieb algebra with parameter $\beta = \rho_k = 2$ here, hence (5.6) is the standard rational solution to (2.6). The same limit is also obtained from the Temperley-Lieb vertex model (2.15)(2.17), for $x = e^{\epsilon u}$, $z = e^{\epsilon/2}$, and $\epsilon \to 0$.

5.4. *Open Questions*

The first question to be answered is whether the solutions (4.50) and their excitations are new. To our knowledge, they are. We can compare them with the Boltzmann weights of the fused 6 Vertex model, which read (in the simplest "2-fused" case of the 19 Vertex model)

$$W_i(x) = 1_i + \frac{x-1}{z - x/z} \left(P_i^{(1)} + \frac{zx - 1}{z^2 - x/z} P_i^{(2)} \right) \tag{5.7}$$

where the P's are unnormalized projectors. We see the emergence of new poles in x, which does not occur in our case. Assuming the models are new, it would also be interesting to find the structure of their fusions, in algebraic terms.

As the model (4.50) is integrable, one should be able to solve it by Bethe Ansatz techniques. The thermodynamic limit will presumably display some interesting phase diagram, of which the second order critical points should correspond to conformal theories. This program will be carried out elsewhere. It would also be desirable to have an elliptic version of the solutions (4.50), generalizing Baxter's 8 vertex model Boltzmann weights.

The 6 vertex model also describes the XXZ quantum spin chain, closely related to the affine sl_2 quantum group. One could wonder whether some "colored" quantum spin chains actually correspond to our models.

Finally, let us recall the connection between Temperley-Lieb algebra and multi-component meanders, established in [9]. A multi-component meander is a configuration of closed non-intersecting loops crossing a line through a given number of points, and may also be viewed as a compactly folded configuration of several possibly interlocked polymer chains. The Fuss-Catalan algebras allow for the definition of multi-colored meanders, with very analogous properties [15].

Acknowledgements

We thank A. Ram for pointing out ref.[10] to us, and P. Pearce for interesting discussions. This work was partly supported by the NSF grant PHY-9722060.

References

[1] R.J. Baxter, *Exactly Solved Models in Statistical Mechanics*, Academic Press, London (1982).

[2] M. Jimbo, *Introduction to the Yang-Baxter equation*, Int. Jour. Mod. Phys. **A4** No.15 (1989) 3759-3777.

[3] G. Delius, M. Gould and Y.-Z. Zhang, *On the construction of trigonometric solutions of the Yang-Baxter equation*, Nucl. Phys. **B432** (1994) 337-403.

[4] M. Jimbo and T. Miwa, *Algebraic analysis of solvable lattice models*, Regional Conference Series in Mathematics, Vol.85, A.M.S. (1994).

[5] H. Temperley and E. Lieb, *Relations between the Percolation and Coloring Problems and other Graph-Theoretical Problems associated with regular Planar Lattices: Some Exact Results for the Percolation Problem*, Proc. Roy. Soc. **A322** (1971) 251-280.

[6] P. Martin, *Potts Models and Related Problems in Statistical Mechanics*, World Scientific, Singapore (1991).

[7] L. Kauffman, *State models and the Jones polynomial*, Topology **26** (1987) 395-407.

[8] P. Di Francesco, O. Golinelli and E. Guitter, *Meander, Folding and Arch Statistics*, Mathl. Comput. Modelling, Vol. **26**, No.8-10 (1997) 97-147.

[9] P. Di Francesco, O. Golinelli and E. Guitter, *Meanders and the Temperley-Lieb Algebra*, Commun. Math. Phys. **186** (1997), 1-59.

[10] D. Bisch and V. Jones, *Algebras associated to intermediate subfactors*, Inv. Math. **128** (1997) 89-157.

[11] M. Jimbo, T. Miwa and M. Okado, *An $A_{n-1}^{(1)}$ family of solvable lattice models*, Mod. Phys. Lett. **B1** (1987) 73-79, and *Solvable lattice models related to the vector representation of classical simple Lie algebras*, Comm. Math. Phys. **116** (1988) 507-525.

[12] V. Pasquier, Nucl. Phys. **B285** (1987) 162-172; J. Phys. **A**:Math.Gen. **20** (1987) L1229, 5707.

[13] P. Roche, Phys. Lett. **B285** (1992) 49-53; S. Warnaar and B. Nienhuis, *Solvable lattice models labelled by Dynkin diagrams*, J. Phys. **A26** (1993) 2301-2316

[14] D. O'Brien and P. Pearce, *Lattice realizations of unitary minimal modular invariant partition functions*, J. Phys. **A28** (1995) 261.

[15] P. Di Francesco and E. Guitter, work in progress.